Semiconductor Terahertz Photonics

Wei-Xin Ni

National Nano Device Laboratories (NDL),
26 Prosperity Rd. I, Hsinchu 30078, Taiwan, R.O.C.

Abstract

The review describes recent advances of research and development on compact semiconductor THz photonic devices, namely quantum cascade laser, especially deals with challenges in device physics, and technical difficulties and possible solutions to fabricate efficient THz laser devices. .

.

1. Introduction

Although there is a great potential for applications in secured communication, high speed wide bandwidth data transmission, remote sensing, medical/bio-medical images, and security surveillance, etc., terahertz (THz) frequencies (0.3 –10 THz), lying between two well-established areas of technology, electronics and optics, remain one of the least studied frequency ranges [1], because lacking of usable device technologies. From the lower-frequency side, conventional electronics keeps pushing upwards. Some device solutions are already able to work up to 400 GHz, however, the maximum electron speed in state-of-the-art semiconductor compounds starts to degrade the electrical performance for frequencies above 500 GHz. At the other side, photonic technologies, in the form of lasers and LEDs, descends to about 10 THz. Thus the frequency range between these two limits has been demoted as the "Teraherz Gap" in the electromagnetic spectrum.

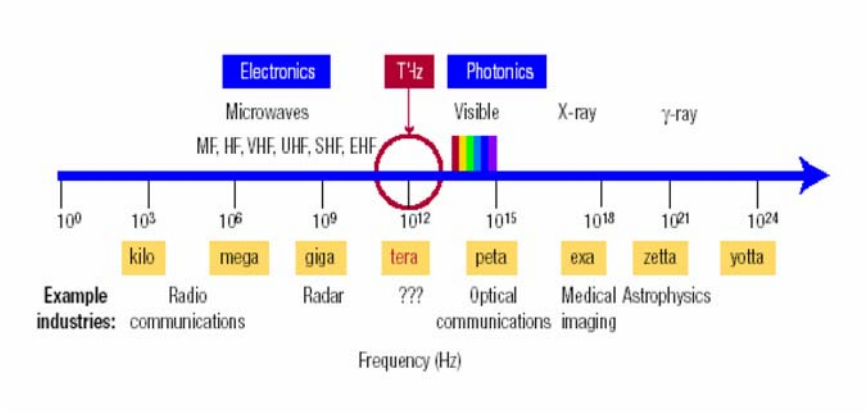

Fig. 1 The THz frequency range

The difficulties when operating electromagnetic devices in the THz frequency range is associated with the propagation length. The physics reason behind is because of drastically increased absorption of the electromagnetic wave at 1-10 THz due to existence of water molecules, as depicted in Fig. 2,. Things always need to be judged from the both sides. Strong water absorption gives restriction for some applications, but on the other hand it may help for other applications

A particularly interesting example is the THz medical and bio-medical image technique [2,3], which could be a sophisticated tool for cancer diagnostics. In contrast to the conventional X-ray images (the image resolutions are in the order of centimetres) relying on the scattering mechanism, the contrast of THz images is created by the water content difference between the ill and healthy part of tissues, such that the millimetre resolution could be achieved (see Fig, 2(a)). This is very crucial for the cancer patients, since the tumour could really be diagnosed at

an early stage for a more effective medication. For the same mechanism, THz waves could been used for detection of bio-chemical agents, such as bacterias or virus, and on-line monitoring of food production, as well..

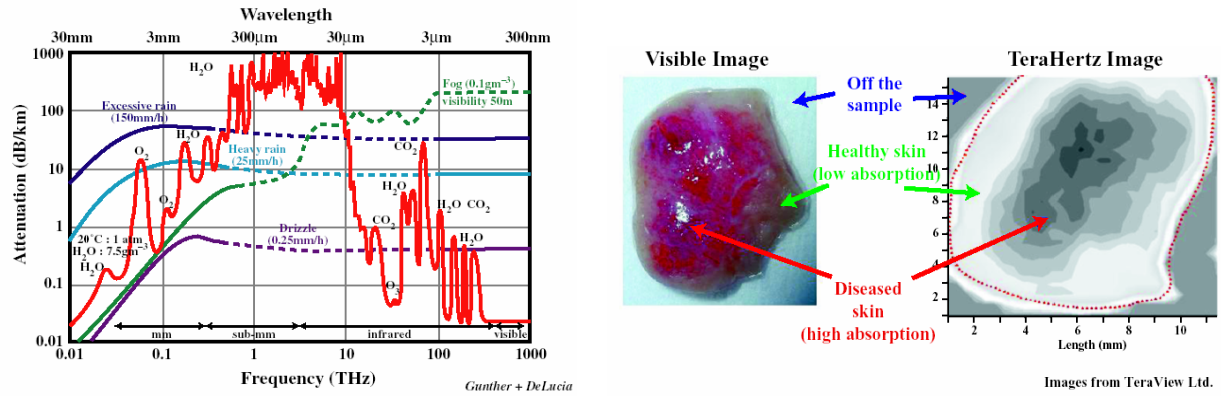

(a) (b)

Fig. 2 (a) The attenuation of electromagnetic wave through air over a wide spectral range. A THz-gap was denoted due to the shortest propagation length. (b) An application example: medical image of skin cancer,

In order to make above-mentioned applications to be feasible, a compact and efficient THz radiation sources is the necessary part. But due to the same reason for a very limited atmospheric propagation length of the electro-magnetic wave, the power generation of THz wave has also been restricted. In recent years, large efforts have been made on the source technology in research in the THz frequencies close to the photonic branch, with the highlight being the development of the THz quantum cascade lasers (QCL) [4-6]. It has therefore caught the attention of the public, and of potential users and investors.

In this paper, a brief overview is given on recent developments of THz photonic sources, with particular addressing of some technological key issues for realizing the compact semiconductor THz source devices, i.e., quantum cascade lasers.

2. Semiconductor THz photonic sources

THz photonic source technologies are in general classified in two groups: (1) Various laser technologies including Free-Flectron Laser for Infrared eXperiments (FELIX)[7], Pulsed THz Laser Systems (operating at a high repetition rate of ~100 MHz)[8], and Continuous-Wave Photomixing Technology[9] (based on THz-wave generation by down-conversion of continuous-wave (cw) laser radiation), etc; and (2) semiconductor-based Solid-State Lasers. The first group requests high investments but still with very lower efficiency values (typically $<10^{-5}$), therefore, only suitable for academic research. The second group is high attractive due to low cost and compactness that can introduce dramatic reductions

in the instrument size and weight, as well as tremendous cost saving when building up a system. However, reliable and efficient compact semiconductor THz laser devices are so far still not available in the market, partly due to material limitations of phonon (relaxation energy of the crystal lattice) bottleneck that blocks the photon emission, since the device must operate at very low energy levels that are in the orders of meV. Therefore, to manufacture an efficient and powerful compact solid source is very crucial for the future of the entire THz technology.

Two types of semiconductor compact laser sources have mainly been studying. One is called resonant state laser (RSL) [10-11] using impurities levels and carries impact ionization effect, therefore, the operation has to be done at very low temperature, below the impurity ionization. Another is QCL, which will be detailed as below.

3 Quantum cascade lasers

QCLs based on intersubband transitions in tailored semiconductor quantum well (QW) structures was first invented and demonstrated by Capasso and co-workers in 1994 at Bell Labs [4,5]. QCLs for the middle infrared range (1-17 μm) are commercially available at present.

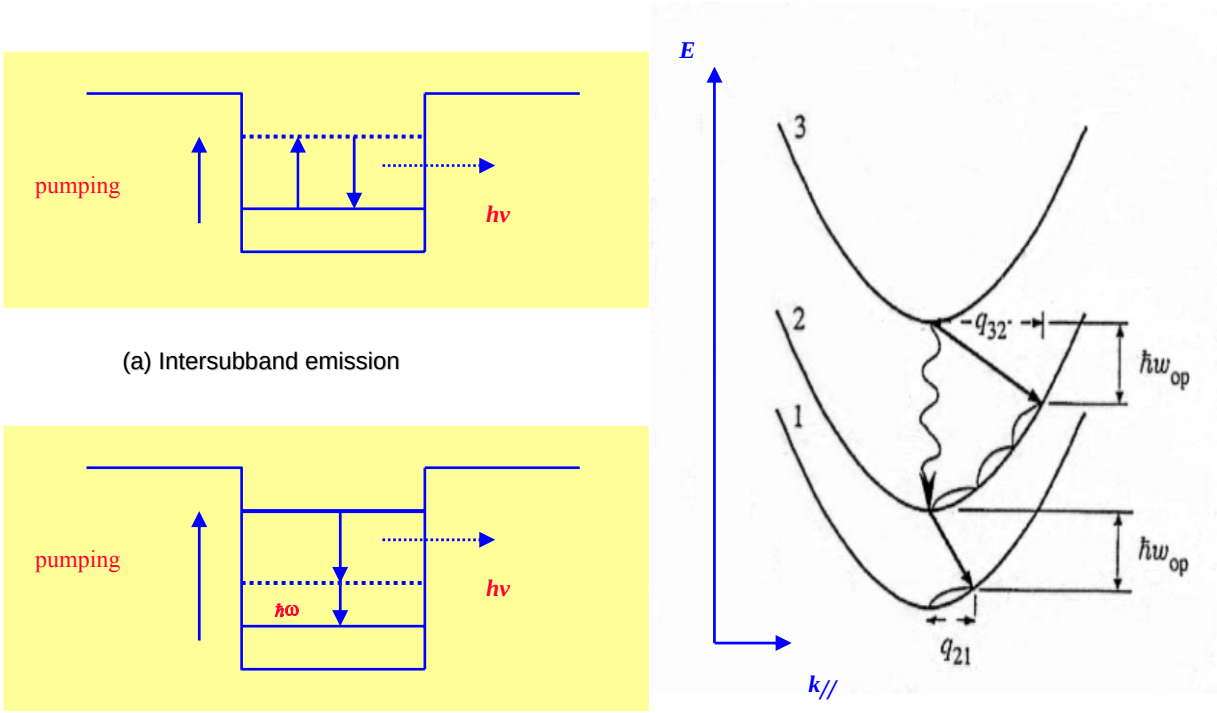

(a) Intersubband emission

(b) Population inversion (3-level syetem)

(c) $r_{LO} \propto (1/q2)$

Fig. 4 Schematic drawing of different processes of intersubband transition in a QW

In contrast to the conventional semiconductor lasers, the QCL is a unipolar device using only electrons or holes for energy transitions between sublevels in a QW. As illustrated in Fig.

4(a), the carriers (electrons or holes) can emit photons by means of intersubband transitions between discrete confined energy levels in the QW. In order to obtain carrier population inversion, one has to design and engineer the QW to involve three sublevels, in which the energy separation between two upper level fits with the desired emitting photon energy while the energy difference between the ground and the first excited states is matching the optical phonon energy (Fig. 4(b)). Since the phonon scattering rate is proportional to $(1/q^2)$, where q is the phonon wave-vector, the transition between level 2 and 1 in Fig 4(c) will be dominated by the fast phonon process, but the transition between levels 3 and 2 will be slow. This is a so-called phonon depopulation mechanism causing carrier population inversion at the level 3, as a basic prerequisite for lasing.

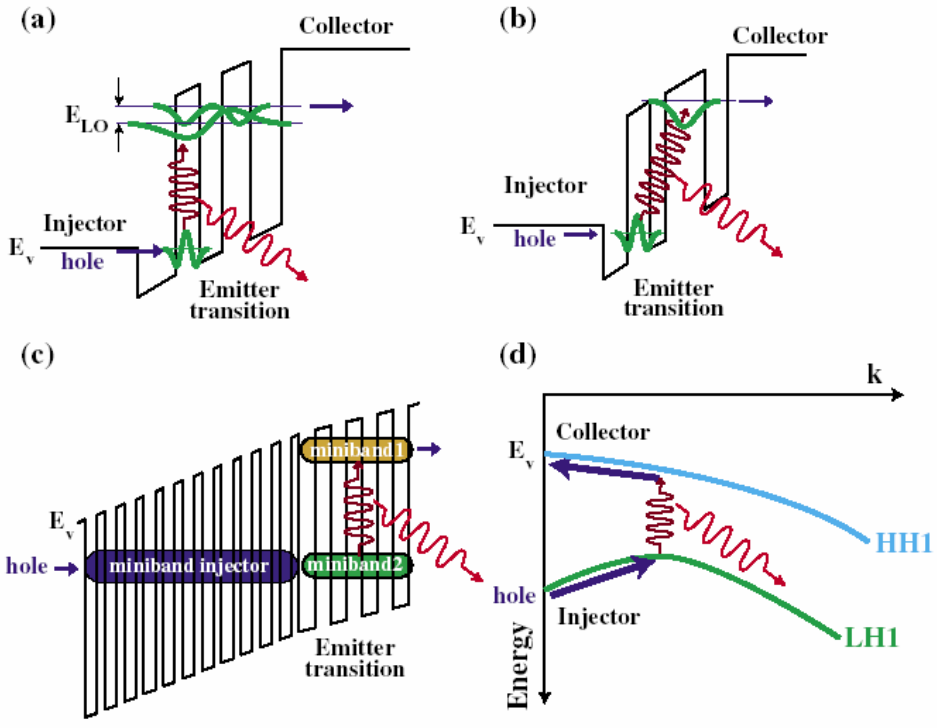

Fig. 5 Schematic diagrams of four possible active regions for a cascade emission device. (a) A vertical transition to hybridised subband levels, with the upper level transaction energy above the optical phonon ($E_{LO}= \hbar\omega_{LO}$) energy in the system (62 meV for Si and 36 for GaAs). (b) A photon assisted transition between subbands in different QWs, (c) Transitions between properly engineered minibands. (d) Transitions between a negative effective mass feature in a light-hole band to a heavy-hole band. Furthermore, the miniband injector can also be used in the active regions of (a), (b), and (d).

By stacking the same QW structures along the growth direction, one carrier can cascade down a series of identical energy steps and emit a photon with the same wavelength at each

step. Thereby, the emitting power of a QCL depends on the number of cascading stages, i.e.,

$$P = N\,(I-I_{th})h/(2e),$$

where N is the number of stages, η is the internal quantum efficiency, I_{th} is the threshold current.

The mechanism is not useful when the emitting photon energy is close to or below the optical phonon energy. Especially, strong non-radiative competition of phonon scattering makes the radiative process very inefficient. This has thus been an inherent problem for III-V semiconductors to produce emission at wavelengths longer than 40 μm, since the material has strong coupling to polar optical phonons ($\hbar\omega_{LO}$=36 meV for GaAs). Other lasing mechanisms or materials should then be considered, in order to manufacture QCLs to operate in the THz wavelength range.

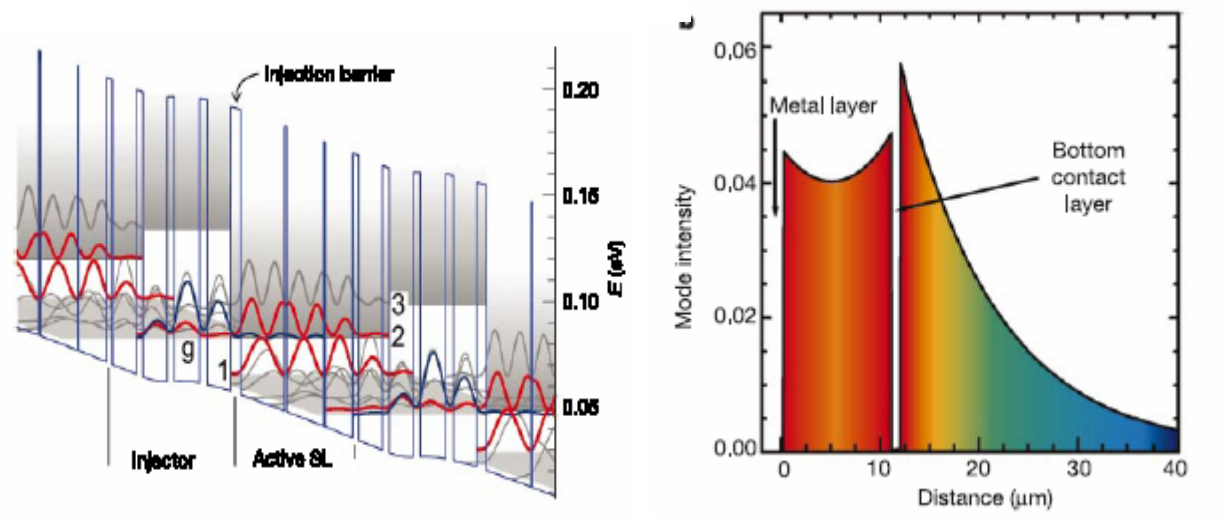

(a) (b)

Fig. 6 (a) Self-consistent calculation of the conduction band structure of a portion of the layer stack in the waveguide core under a field of 3.5 kV cm^{-1}. Injectors and superlattice (SL) active regions are alternating. (b) Calculated mode profile along the growth direction of the final device structure. The origin of the abscissa is at the top metal/semiconductor interface, and the waveguide core of the superlattice active region is between the bottom contact and top metal layer.

Several possible mechanisms for THz lasing using subband engineering are summarized in Fig. 5. To find a proper way to depopulate the lower band while suppressing the thermal backfilling are the main concerns for a successful QC laser structure. The mechanism (c) has

been successfully used nowadays in the design of GaAs/AlGaAs-based QC lasers operated between 4.4-2.3 THz, and the mechanism (c) is favored for SiGe/Si based QC structures, as will be discussed in more detail in the following subsections.

3.1 QCLs based on GaAs/AlGaAs heterostructure materials

In the work carried out within the EU supported collaborative project WATED, Köhler et al. [6] have fabricated a QCL using a rather complicated design of miniband QW structures grown by MBE. By fabricating mirrors using mechanical cleaving and waveguide introduced by the plasmon boundary condition due to metal and n+ layers on both sides of the active region, laser spectra were obtained at 4.4 THz (67 μm) [6], 3.4 THz (80 μm) [12], 3.5 THz (86 μm) [13], and very recently 2.3 THz (127 μm) [14], respectively.

The keys to achieving lasing from these quantum cascade structures are summarized in the following. (1) The proper design of the multi-quantum-well module in the active region is essential, such that the lower laser state 1 in Fig. 6(a) is strongly coupled to a wide injector miniband. The electrons emit photons on undergoing transitions between levels 2 and 1 of the active region, and subsequently enter the successive injector region ensuring fast depletion of state 1. (2) The wide miniband in the injector region, comprising seven sub-bands spanning an energy up to 17 meV, allows efficient electrical transport, even at high current densities, and simultaneously suppressing thermal backfilling. (3) The waveguide is a very important aspect of the QC laser device. In order to achieve a tight optical confinement with low absorption losses, double-surface plasmon structures have been considered with one at the upper metal/semiconductor interface with dielectric constants of opposite sign, and another one is a thin (800 nm) n^+-GaAs layer between the active superlattice region and an undoped GaAs substrate, as depicted in Fig. 6(b).

For the a 1.96 mm long and 150 μm wide QC laser operated at ~4.4 THz, collected (with 33% efficiency of mirrors) CW output powers of 4 mW per facet are measured at liquid helium temperatures, and a maximum operating temperature of 48 K is reached [15], as shown in Fig. 3.6(b). Under pulsed excitation at duty cycles of 0.5%–1%, slightly higher (10%) peak powers are reached, and the device can be operated up to 67 K. Low threshold current densities of 165 and 185 Acm^{-2} are observed in pulsed and CW operation, respectively. For the devices operated at ~ 3.5 THz, the maximum measured peak output power is ~ 2.5 mW at 5K, and laser action is obtained in pulsed mode at temperatures up to 65 K, and at 50% duty cycle up to 29 K [12]. CW output powers of a few hundred microwatts are estimated at low temperatures [13]. Furthermore, record low-threshold-current densities of 95 and 115 A cm^{-2} were observed in pulsed and CW operation, respectively [16].

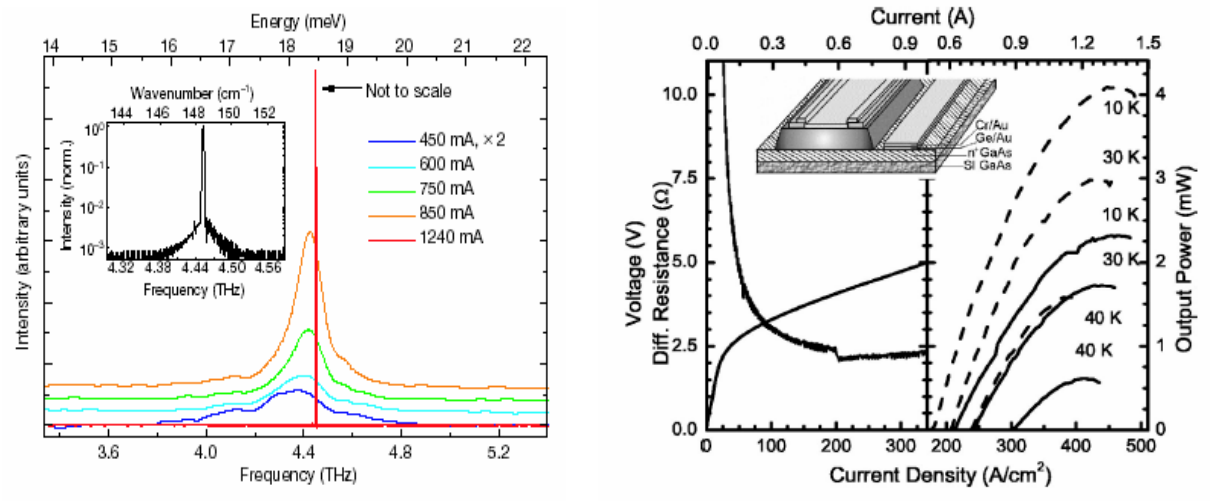

Fig. 7 (a) Emission spectra from a 1.24 mm long and 180 μm wide laser device recorded at 8 K for different drive currents. It is evident that a dramatic narrowing of the spectral line width was observed above the lasing current threshold of 1.24 A at 4.45 THz. (b) *L* – *I* and *V*– *I* characteristics of a 1.96 mm long and 150 μm wide laser stripe are plotted in solid lines, while the CW power values (from one facet) vs. the injection current are plotted at the right part of the figure at different heat sink temperatures ranging from 10 – 40 K.

3.2 QCLs based on Si/SiGe heterostructure materials

Traditionally, in the realm of optoelectronics, Si-based materials are not considered to be very useful, because of the indirect bandgap. However, the intersubband transitions in Si-based QW structures are not forbidden by the k-selection rules, therefore, they are proposed for fabrication of QCLs [16]. There are even several distinct advantages, which make Si/SiGe heterostructures very interesting for applications in THz QCL devices:

- The mature processing technology - Si CMOS ICs, so production costs are ≤1/10 of GaAs technology.
- The lack of strong phonon scattering mechanisms (polar optical phonon) allows higher emission efficiency and operating temperatureA good thermal conductivity (~3 times higher than GaAs) helps CW mode operation at room temperature

So far, there is no report on Si/SiGe QC lasers, but several groups have demonstrated cascade devices for spontaneous emission, e.g., Si/SiGe cascade LEDs at 103 μm (2.8 THz) [20,21], 50 μm (7 THz) [19], 37 μm (8.1 THz) [20], and 9.5 μm (31.4 THz) [21], respectively.

A special feature of the Si/SiGe heterostructure system is that the band structures can be tailored by manipulating the strain condition of the layer structure. Theoretically it has been predicted that there may exist an inverted effective mass in the splitted light hole band at $k_{//}$=0

when a strain symmetrized SiGe multi-QW structure or superlattice is grown on a virtual substrate [22], which in turn results in a four-level system for transitions between the light-hole and heavy-hole subbands in SiGe QWs, as shown in Fig. 3.3(d), enabling population inversion and a very high optical gain.

The main technical challenge to achieve an efficient Si-based THz emitter is still associated with the materials research, i.e., how to grow a high quality, thick (demanded for the mode confinement), and strain compensated Si/SiGe multi-QW structure with a high number of periods (> 100 repeated QC modules) on a SiGe virtual substrate. At the same time, there are also needs to study the physical properties of various designed structures, in order to gain proper knowledge that is needed for the engineering work of the efficient Si-based solid THz devices.

Several attempts towards the first Si/SiGe THz quantum cascade laser have been made by researchers from Linkoping University in Sweden, Johannes Kepler Universität at Linz in Austria, and University of Cambridge and Heriot-Watt University in UK with an EU-FET project SHINE. Some results are summarized below.

In order to overcome the inherent difficulty that the thickness of epi-growth is limited by the huge lattice-mismatch between Si and SiGe, while successful laser devices require a thick active region (normally >> 1 μm) to obtain high enough optical gain, the solution is the growth of strain-symmetrized Si/SiGe superlattice structures on relaxed SiGe virtual substrates. Essentially defect-free thick layers with abrupt heterojunction interfaces were obtained, while low-temperature growth was considered as a key to address above issues [18].

The first design was based a Si/SiGe supperlattice structure contained 100 periods of 2.2 nm-Si/4.4 nm-$Si_{0.7}Ge_{0.3}$ grown on the $Si_{0.8}Ge_{0.2}$ virtual substrate at ~ 350 °C as the active region. For this structure, the injected holes could decay faster from light hole1 (LH1) to the heavy hole1 (HH1) subbands in the SiGe quantum well. Optical emission was then expected during a slower transition via tunneling process between the HH1 and LH1 subbands in adjacent SiGe quantum wells. Such an interwell transition is called ‘diagonal transition’, and according to Kelsall’s theoretical work it may give rise the emission peaked at ~3 THz [9].

Shown in Fig. 8(a) are the ω-2θ scan of high-resolution X-ray diffraction (HRXRD). together with dynamic simulations performed using the Philips X’pert Epitaxy software that is based on the Takagi-Taupin equations. No fitting was made beween these two curves,, indicating the growth was well controlled. The samples were then processed into 200×200 μm^2 mesas, with top and back contacts for vertical current injection.

The electroluminescence measurements were performed using a fourier transform infrared spectroscopy (FTIR) with a cooled Si bolometer. Typical spectra under 7.5 V bias and 960 mA injection current with 10% duty cycle are shown in Fig. 8(b). An emission peak at ~13 meV (~3 THz) can be observed with a rather constant intensity and energy position at both 4.2 K and 40 K, which is consistent with the theoretical prediction and experimental observation of the HH1 to LH1 interwell intersubband transition [9].

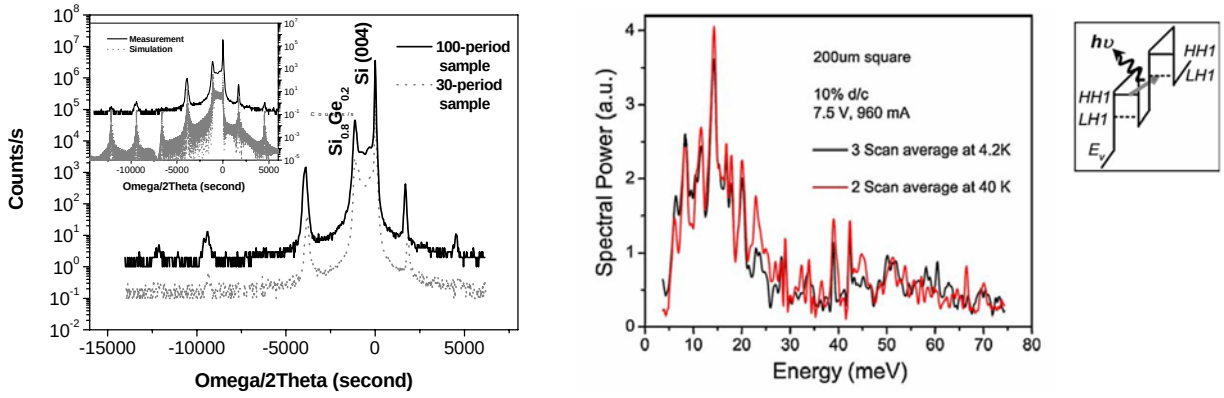

(a) (b)

Fig. 8. (a) (004) ω-2θ rocking curves of two Si/SiGe QC samples. The comparison between simulation and measurement curve for the 100-period sample is shown in the inset. (b) FTIR electroluminescence spectra at 4.2 K and 40 K, and the expected optical transition is illustrated in the potential diagram in the insert

In order to further solve the problems of the high electric fields in the phonon depopulation designs, it was clear that a structure with a number of QWs designed to produce a miniband was a good way forward to get to low electric fields to reduce heating. Therefore bound-to-continuum designs similar to those for GaAs THz QCLs [15] were considered. The idea of the bound-to-continuum is that holes are injected into an isolated upper state created inside the minigap by a QW beside the injection barrier while hole extraction occurs through a lower miniband. The diagonal nature of the radiative transition results in a high upper state lifetime and helps to maximise population inversion and injection efficiency while the miniband is used to extract the holes to reduce the lower state population.

Fig. 9 shows one structural design, which has a 3.7 nm injection barrier with the bound state in the QW at 135 nm and the transition is to three states in the QWs at 140 nm which are part of the miniband. The design is strain-symmetrised on a $Si_{0.8}Ge_{0.2}$ virtual substrate with strained-Si barriers and $Si_{0.724}Ge_{0.276}$ QWs. The electric field has been reduced to 7 kV/cm for a 26.4 meV transition [23].

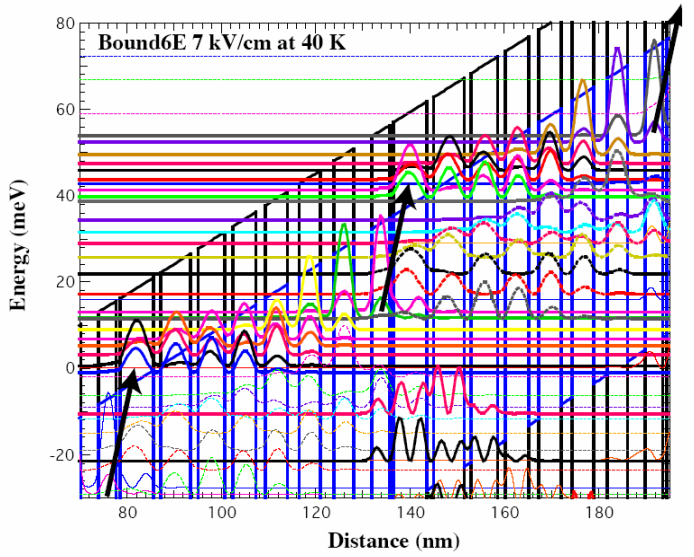

Fig. 9 A Si/SiGe bound-to-continuum cascade design showing the square of the envelope functions as calculated by -band **k.p** theory. The transition energy is 2 meV and the miniband width is 12. meV. Holes flow up the page to lower hole energy i.e. the valence band is at the top of the page. The solid envelope functions are HH states while the dashed states are mixed LH/SO states. The arrows indicate the radiative transition.

Such a strain-symmetrized Si/SiGe bound-to-continuum QC structure has recently successfully on a fully relaxed SiGe virtual substrate using solid-source MBE at a substrate temperature of 330 °C at Linköping [24], although it was a very challenging. The while design was complex, and the required structure contained 20 periods of active units with 405 layers, in which the thinnest layer was only 0.8 nm while the total thickness was over 2μm.

The samples were characterized by using atomic force microscopy (AFM), high resolution X-ray diffraction (HRXRD), and transmission electron microscopy (TEM). AFM images showed r.m.s. values in the order of 2-3 nm, while the strain condition, the abruptness of heterojunction interfaces, and the thickness uniformity over such a thick sample were evidenced by cross-sectional TEM (Fig. 10). The structure is now underway being processed as waveguided devices for emission measurements.

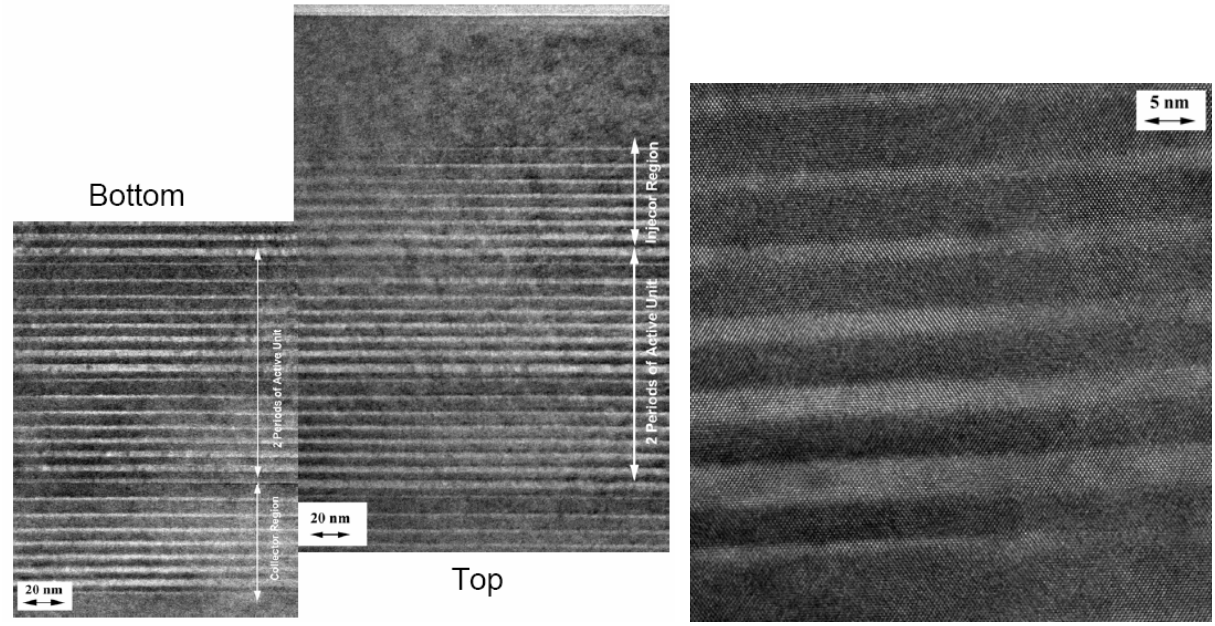

(a) (b)

Fig. 11 XTEM microgphs of a bound-to-continuum QC sample. (a) shows the thickness uniformity of top and bottom parts of the sample, and (b) is the high-resolution lattice image revealing sharp interfaces.

An important issue is that whether the lifetime of the interwell intersubband transition across a Si barrier would satisfy the lasing requirement, and how it could be engineered in order to obtained the desired structure. Time-resolved pump-probe spectroscopic measurements using Dutch far-infrared free electron laser FELIX with micro-pulse width of ~ 5ps were carried out [25] for a group of QW structures with various thickness designs of the barrier and well layers. It was found that the typical decay time of the LH1-HH1 intersubband relaxation within the well was ~20 ps, but this decay time became very short (few picoseconds) [26] when the hole temperature was elevated. Furthermore, a lifetime increase by a factor of 2 (~40 ps) was observed for samples with very narrow SiGe QW (< 4 nm) or Si barriers, which was attributed to the broadening of LH1 state wavefunction with spatial extent into the barriers. Such delocalization behavior is believed to transfer holes to the states across the Si barrier layer [27]. It was therefore demonstrated that this “diagonal transport” in mid-infrared SiGe QC structures increases significantly the corresponding carrier lifetime up to several hundreds ps . Furthermore, the effectively decay time remained constant from 4 to 100 K, which was substantially different to the GaAs/AlGaAs system where the lifetimes are strongly dependent on temperature above 35 K due to polar optical phonon scattering,. These data thus indicate that Si-based materials are still being promising for applications in THz photonics, especially in terms of thermal properties mad temperature dependent performance.

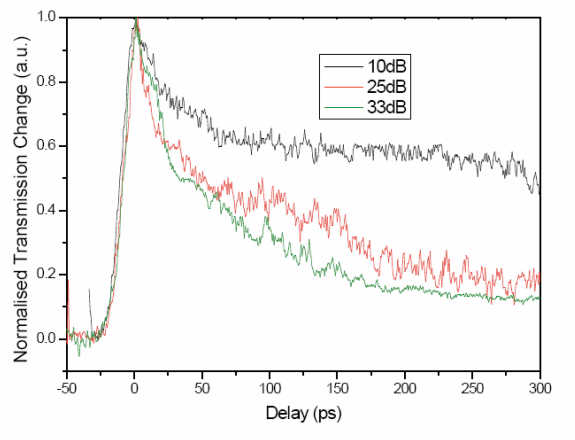

Fig. 11 Normalized probe transmission change against delay time at four different pump intensities (λ=37 μm) for sample 2 at 4 K

4. Conclusion

In conclusion, THz technology may bring a lot of new applications in the future, but the bottleneck at moment is the emission sources. Quantum cascade structures are very promising and lasers have been successfully fabricated using III-V semiconductors. For the Si/SiGe materials, although there are several distinct advantages for THz applications, the supply of high quality material remains difficulties for laser devices. More efforts are demanded in order to demonstrate a Si/SiGe quantum cascade laser..

Acknowledgement

The Si/SiGe QC emitter work has been supported by grants from the EU project SHINE (IST-2001-38035), and Swedish defense-related nano research program (F-NANO).

References

[1] P. H. Siegel, IEEE Tr. on Microwave Theory and Techniques, vol. 50, pp. 910-928, 2002.
[2] D.D. Arnone, C.M. Ciesla and M. Pepper, Phys. World **13**(4), 35 (April 2000)
[3] R.M. Woodward, B. Cole, V.P. Wallace, D.D. Arnone, R. Pye, E.H. Linfield, M. Pepper and A.G. Davies, Proc. CLEO Paper CWE4 (2001)
[4] J. Faist, F. Capasso, D.L. Sivco, C. Sirtori, A.L. Hutchinson, and A.Y. Cho, Science 264, 553 (1994).
[5] F. Capasso, R. Colombelli, R. Paiella, C. Gmachl, A. Tredicucci, D.L. Sivco, and A.Y. Cho, Opt. Photon. News, vol. 12, no. 5, p. 40, May 2001.
[6] R. Köhler, A. Tredicucci, F. Beltram, H.E. Beere, E.H. Linfield, A. G. Davies, D.A. Ritchie, R.C. Iotti, and F. Rossi, Nature 417, 159 (2002).
[7] S.V. Benson, ‚Optics & Photonics News, vol.21, no. 5, p. 20-, May 2003.
[8] E. Mueller, Coherent-DEOS white paper.
[9] K.Siebert, H. Quast, H. Rostmos, Proc. of International THz Workshop 2000, p. 24, Sandbjerg, Denmark.
[10] I. V. Altukhov, M. S. Kagan, K. A. Korolev, V. P. Sinis, E. G. Chirkova, M. A. Odnoblyudov and I. N. Yassievich, JETP 88, 51 (1999).
[11] E. Brundermanna, D.R. Chamberlin, and E.E. Haller, Apl. Phys. Lett. 76, 2992 (2000).
[12] B.S. Williams, H. Callebaut, S. Kumar, Q. Hu, and J.L. Reno, Appl. Phys. Lett. 82, 1015 (2003).
[13] R. Köhler, A. Tredicucci, F. Beltram, H.E. Beere, E.H. Linfield, A.G. Davies, and D.A. Ritchie, Optics Lett. 28, 810 (2003).
[14] D.A. Ritchie, private communications..
[15] R. Köhler, A. Tredicucci, F. Beltram, H.E. Beere, E.H. Linfield, A. G. Davies, D.A. Ritchie, S.S. Dhillon and C. Sirtori, Appl. Phys. Lett. 82, 1518 (2003).
[16] R.A. Soref, L. Friedman and G. Sun, Superlattices and Microstructures" 23, 427 (1998)
[17] R.W. Kelsall, D.J. Paul, S.A. Lynch, R. Bates, Z. Ikonic, P. Harrison, D.J. Norris, A.G. Cullis, D.D. Arnone, P. Murzyn, A. Loudon and C.R. Pidgeon, DARPA THz Review Meeting, Colorado Springs, USA, August 2001.
[18] M. Zhao, w.-x. Ni, p. Townsend, S.A. Lynch, D.J. Paul, C.C. Hsu, M.N. Chang, Thin Solid Films 508, 24 (2006).
[19] S.A. Lynch, S.S. Dhillon, R. Bates, D.J. Paul, D.D. Arnone, D.J. Robbins, Z. Ikonic, R.W. Kelsall, P. Harrison, D.J. Norris, A.G. Cullis, C.R. Pidgeon, P. Murzyn and A.Loudon,]Material Science and Engineering B89, 10 (2002).
[20] R.T. Troeger, T.N. Adam, S.K. Ray, P.C. Lv, U. Lehmann and J. Kolodzey, in Symposium M, Progress in Semiconductor Materials II--Electronic and Optoelectronic Applications, M2.4, MRS Fall Meeting, Boston, 2002.

[21] G. Dehlinger, L. Diehl, U. Gennser, H. Sigg, J. Faist, K. Ensslin, D. Grützmacher and E. Müller, Science 270, 2277 (2000).
[22] G. Sun, L. Friedman and R. A. Soref, Phys. Rev. B62, 8114 (2000).
[23] D. J. Paul, P. Townsend, S.A. Linch, M. Zhao, W.-X. Ni, the 3rd International Silicon-Germanium Device and Technology Meeting (ISTDM-3, Princeton, May 15 -17, 2006),
[24] M. Zhao and W.-X. Ni, to be published.
[25] C.R. Pidgeon, P.J. Phillips, D. Carder, B.N. Murdin, T. Fromhertz, D.J. Paul, W.-X. Ni and M. Zhao, Semicond. Sci. Technol., 20, L50. (2005)/
[26] R.W. Kelsall, Z. Ikonic, P. Murzyn, C.R. Pidgeon, P.J. Phillips, D. Carder, P. Harrison, S.A. Lynch, P. Townsend, D.J. Paul, S.L. Liew, D.J. Norris, and A.G. Cullis, Phys. Rev. B, 71, 115326 (2005).
[27] M. Zhao, A. Karim, W.-X. Ni, C. R. Pidgeon, P. J. Phillips, D. Carder, B. N. Murdin, T. Fromherz, D. J. Paul , accepted by J. Luminescence.